Schlieren Image Velocimetry and colorimetry for a burning candle and its thermal plume

Raluca Andreea ROSU*

*Corresponding author
UNSTP – National University for Science and Technology POLITEHNICA Bucharest, Faculty of Aerospace Engineering,
Splaiul Independentei 313, 060042, Bucharest, Romania,
raluca797@gmail.com

DOI: 10.13111/2066-8201.2024.16.3.10

Received: 02 July 2024/ Accepted: 02 August 2024/ Published: September 2024

Abstract: *This article explores the feasibility of generating velocity maps for a flame and its plume from a burning candle using Schlieren Image Velocimetry (SIV). Currently, SIV is predominantly employed in the literature to track highly turbulent flows by using the developing eddies as flow markers. The novelty of this study lies in evaluating the quality of a nearly laminar flame, which exhibits significant background density variation due to its own plume. In addition to the SIV technique, a brief assessment is conducted using a segmented color filter, specially designed and manufactured to evaluate the potential for measuring the temperature range of the flame.*

Key Words*: SIV, Particle Image Velocimetry (PIV), calibrated color filter schlieren, Image Post-Processing, high temperature flame*

1. INTRODUCTION

In fluid dynamics research, schlieren techniques are pivotal for visualizing and quantifying density gradients within fluids using advanced optical setups. Settles [1] and Schmidt [2] extensively describe configurations that employ curved mirrors to discern subtle variations in fluid density. These setups leverage the principles of light refraction through the fluid medium, enabling a precise visualization of density gradients. This capability facilitates the observation and analysis of phenomena such as heat transfer and acoustic waves [1, 2]. The test area provided by the single-mirror technique is very narrow, and if not at a precise focal point, being even slightly too close can result in a doubled image. In contrast, the Z-type two-mirror configuration, explored by Prisacariu et al. [3], enhances spatial resolution and sensitivity. This setup involves two parabolic mirrors arranged in a specific geometry to improve the visualization of subtle density gradients. By precisely aligning the mirrors, it enables detailed studies of complex flow patterns and disturbances in fluid media. Schardin [4] and Meier [5] provide foundational insights into the quantitative evaluation and application of schlieren methods. Schardin's work on the principles of schlieren imaging emphasizes its utility in quantitatively assessing density gradients. Meier's background schlieren technique, although not specific to the single-mirror or Z-type configurations, contributes to the overall understanding of how optical methods can be adapted and optimized for different experimental needs in fluid dynamics research. Comparatively, the single-mirror configuration excels in

simplicity and cost-effectiveness, making it accessible for basic fluid density visualization studies [1, 2]. It provides qualitative data on density gradients but may lack the precision and spatial resolution of more complex setups like the Z-type configuration. On the other hand, the Z-type two-mirror configuration [3] offers enhanced spatial resolution and sensitivity, suitable for capturing detailed flow structures and subtle density changes. This setup is advantageous in studies requiring precise measurements and detailed visualization of flow phenomena, such as turbulent flows and aerodynamic studies.

Rainbow schlieren techniques, as explored by Howes [6] and Agrawal et al. [7], provide advanced capabilities in visualizing and quantifying density variations in fluid flows. Howes's research highlights the versatility and applications of rainbow schlieren in fluid dynamics research, showcasing its effectiveness in studying complex flow behaviors. Agrawal et al. further extend this capability by demonstrating three-dimensional rainbow schlieren tomography, which offers precise measurements of temperature fields and density gradients in gas flows. Experimental Fluid Mechanics, as comprehensively covered by Adrian et al. [8], provides essential knowledge on various experimental techniques in fluid mechanics, including schlieren methods. This reference serves as a foundational textbook for understanding the principles and applications of schlieren in diverse research domains. Settles and Jonassen [9] introduce Schlieren Particle Image Velocimetry (PIV) for turbulent flow studies, showcasing its utility in quantifying flow dynamics and density variations. Their work demonstrates the evolving applications of schlieren techniques in capturing and analysing turbulent flow behaviors. Philpott's [10] development of a variable sensitivity and orientation color schlieren system adds another dimension to the technique's versatility, allowing for enhanced differentiation of density gradients in complex flow environments. This method provides greater flexibility and precision in visualizing and quantifying flow phenomena, making it a valuable tool for advanced fluid dynamics research. In their study on the temperature measurement of fluid flow using a focusing schlieren method, Martínez-González et al. [11] provide valuable insights into the application of schlieren techniques for detailed thermal analysis. Their methodology, which accurately captures planar temperature fields, can be instrumental in enhancing the precision of temperature measurements in the thermal plume of a burning candle. By adopting and adapting their focusing schlieren approach, my research on Schlieren Image Velocimetry and colorimetry can benefit from improved spatial resolution and sensitivity, enabling a more comprehensive visualization and understanding of the complex flow and thermal dynamics involved.

In the study of segmented filters and background-oriented schlieren (BOS) techniques, the application of Kodak Wratten gelatin filters [12] enables precise measurement of displacement and dynamic range in schlieren imaging. The segmented filter, using RGB color ratios, allows for the calculation of the source image's position and has a defined range and sensitivity based on the source size. In contrast, the BOS setup simplifies optical components and utilizes a random dot pattern for illumination, with the ability to measure displacements in both PIV and schlieren modes. The PIV-mode, with fewer components, focuses on a background pattern for displacement measurement, while the schlieren-mode enhances resolution by maintaining nearly parallel light rays, thus minimizing scaling errors. These methods' detailed measurements and adaptability to different configurations contribute significantly to capturing accurate flow and density gradients in optical experiments [13].

In their comprehensive study on quantitative schlieren methods, Elsinga et al. [14] offer a detailed assessment of both calibrated color schlieren and background oriented schlieren techniques. Their work highlights the application of these methods in providing accurate and high-resolution measurements of fluid flows. This study's insights into calibration and

application can significantly enhance my research on Schlieren Image Velocimetry and colorimetry by offering proven techniques for improving measurement accuracy and dynamic range. By leveraging their findings, my research can adopt refined calibration procedures and more effective background-oriented schlieren techniques, leading to enhanced visualization and analysis of the thermal plume and flow dynamics associated with a burning candle.

Prisăcariu and Prisecaru [15] provide a thorough exploration of schlieren image velocimetry methods applied to a round, hot, turbulent air-jet in their recent publication. Their study emphasizes advanced techniques for capturing the complex dynamics of turbulent flows, offering valuable insights into the measurement of velocity fields and the behavior of high-temperature jets. By incorporating their methodologies and findings, my research on Schlieren Image Velocimetry and colorimetry can benefit from enhanced techniques for analyzing turbulent flow structures and thermal plumes. Their work on optimizing image processing and analysis for turbulent air-jets will aid in refining the precision and accuracy of measurements in the thermal plume of a burning candle.

Particle Image Velocimetry: A Practical Guide [16] serves as an essential reference for mastering the principles and advanced applications of PIV, offering comprehensive insights into the methodologies and parameters crucial for accurate flow visualization. This authoritative guide, combined with the instructional clarity of Thielicke's tutorials [17], has significantly informed the processing and analysis of schlieren images using PIVLab in Matlab. These resources together provide a robust foundation for optimizing image processing parameters, ensuring precise and reliable results in the study of fluid dynamics.

The present paper focuses on the study of a nearly laminar candle flame, employing a Z-type schlieren setup with an integrated color filter. This color filter is utilized both in the images acquired for Schlieren Image Velocimetry (SIV) analysis and for temperature range measurement. Compared to other studies that focus on flame characterization through Schlieren techniques, the current study offers a unique perspective by addressing the challenges associated with analyzing a nearly laminar flame. Unlike the more turbulent flames typically examined with Schlieren methods, the nearly laminar flame studied here presents a relatively stable flow with subtle density variations, primarily influenced by the flame's own plume. This allows for a more refined examination of flow dynamics and temperature distributions. The integration of a segmented color filter, specifically tailored for temperature range measurement, further enhances the analytical capability, providing a dual-function approach that simultaneously captures detailed velocity maps through SIV and temperature variations within the flame. Additionally, the paper includes the post-processing of Schlieren images using Matlab, incorporating both the PIVLab add-on and custom codes. Various parameters such as window size, overlap, and correlation methods are explored to optimize the accuracy and resolution of velocity fields, temperature distributions, and derivative parameter maps. This combined methodology not only broadens the application of Schlieren imaging in less turbulent scenarios but also contributes to a deeper understanding of laminar flame behavior, potentially influencing future flame characterization techniques.

2. EXPERIMENTAL SETUP

The experiment was conducted to study the temperature gradient of a candle flame using a color segmented filter in conjunction with a Z-type configuration schlieren method. This setup allows for the precise visualization of temperature variations within the flame, utilizing a high-speed camera and specially designed optical components to capture detailed schlieren images. The color linear filter enhances the ability to distinguish temperature differences by converting

refractive index changes into color variations, thereby providing a clear and accurate representation of the thermal gradients present in the candle flame.

Initially, a qualitative imaging session was performed to analyze and select the filter that effectively reveals deflected light rays, allowing for a visible observation of the density gradient distribution. The images captured during this session are shown in Fig. 1.

a) b) c)

Fig. 1 – Images of several quantitative flames images, with the applied filter: a) flame in laminar state with half-blue filter, b) flame with half yellow – half green filter, c) multi-color filter applied to the flame

The propagation of the phenomenon in a laminar state proves to be happening in a very small area.

For the system to be sensitive enough to capture different gradients in that state, a very small light source should be passing a filter with multiple colors. In that case, the filter fringes should alternate at micronic level, which is not applicable at the moment, to the studied case.

The configuration of the experimental setup used for this study is depicted in Fig. 2.

The point light source emits light that is initially divergent. The light first travels towards the first parabolic mirror. This mirror collimates the divergent light into a parallel beam. Collimation means the light rays are made parallel, which helps in creating a sharp and clear schlieren image. The first parabolic mirror captures the divergent light from the point source and reflects it as a parallel beam towards the test area. The shape of the mirror ensures that all the rays converge to the focal point.

The collimated light beam passes through the test area where the candle flame is located. As the light travels through the thermal plume and surrounding air, it encounters regions of varying density due to the heat emitted by the candle. These density variations cause the light to bend or refract.

The areas with different temperatures or densities alter the light path differently, leading to changes in the light beam's intensity and direction. After passing through the test area, the light beam is captured by the second parabolic mirror. This mirror reflects and refocuses the parallel light beams that have been altered by the density gradients in the test area. The second parabolic mirror directs the light towards the camera.

This refocusing helps in forming the schlieren image by translating the variations in light path (caused by refraction) into visible contrasts. The filter is used to enhance the contrast of the image by blocking or modulating certain parts of the light spectrum, making the density variations more visible in the final image. The camera captures the schlieren image formed by the refocused and filtered light. The resulting image displays variations in light intensity that correspond to the density gradients within the test area. These variations are visualized as dark and light regions, revealing the structure and behavior of the thermal plume or flow.

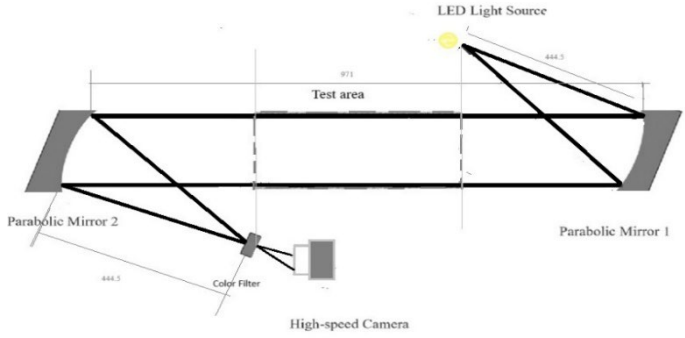

Fig. 2 – Optical configuration of the Z-type schlieren system

The optical path and equipment configuration allow for the visualization of these gradients with minimal optical errors, despite the off-axis mirror angle being set in the picture 10°, exceeding the typical 3°. The angle it's exaggerated in order to better fit the equipment in the sketch. All distances are measured in millimeters. To provide a comprehensive overview of the experimental setup utilized in this study, a detailed description of the equipment is presented in Table 1.

Table 1. Schlieren equipment specification

Type of equipment	Name	Specification
parabolic twin mirrors	Al-plated, Edmund Optics	Effective focal length=1524mm
high-speed camera	Phantom VEO 710L CMOS sensor	12-bit per color Resolution:912x552 Acquisition speed: 7500fps
color filter	Filter	Segmented
candle	White wax candle	Paraffin wax candle Diameter 66.62 mm
light source	LS-W1	Laser pumped,500 mW Optical fiber, round, 1mm diameter

The color succession of the filter's fringes can be observed in Fig. 3. This filter is the one used to capture the images on which the quantitative analysis has been achieved.

Fig. 3 – Real arrangement of the color schlieren filter fringes

To complement the segmented color filter photo used in the thermal analysis, a table is provided below detailing the dimensions of each color band within the filter. Table 2 outlines the specific ranges of the temperature bands as assigned by the filter's color segments. Each segment represents a distinct temperature range, allowing for precise mapping and analysis of temperature distributions within the thermal plume.

Table 2. Magnification factor for the segmented color fringes displayed in Fig. 3.

No.	Color gradient	Dimension [mm]	Position (left to right)
1.	aqua blue	0.96875	1
2.	yellow	1.4375	2
3.	light pink	1.125	3
4.	pink	1.21875	4
5.	orange	0.96875	5
6.	light pink	1.15625	6
7.	dark purple	1.15625	7
8.	blue	1.125	8
9.	green	1.125	9
10.	yellow	1.09375	10
11.	pale pink	1.09375	11
12.	dark red	1.1875	12
13.	light blue	1.6875	13
14.	dark blue	0.9375	14
15.	dark green	1.125	15
16.	scarlet red	1.08	16

This experiment is designed to study the Z-type schlieren color imaging technique, focusing on optimizing its application for analyzing fluid dynamics and temperature distributions. To advance the analysis of the captured fluid dynamics and generate a detailed temperature map of the candle flame, various parameters such as window size, overlap, and interpolation methods must be optimized in PIVlab. This optimization will enhance the accuracy of velocity field measurements while also facilitating the integration of schlieren data for precise temperature mapping. By carefully selecting and adjusting these parameters, the schlieren images can be effectively processed to reveal both the fluid dynamics and temperature distribution within the candle's flame and its thermal plume.

Using the setup depicted in Fig. 2 with the filter from Fig. 3, taking into account the specific parameters found in Table 1, the images of the phenomenon have been recorded.

3. POST PROCESSING OF THE SCHLIEREN IMAGES

The recorded image sequence can be found in Fig. 4 and it represents the analysed phenomenon frames.

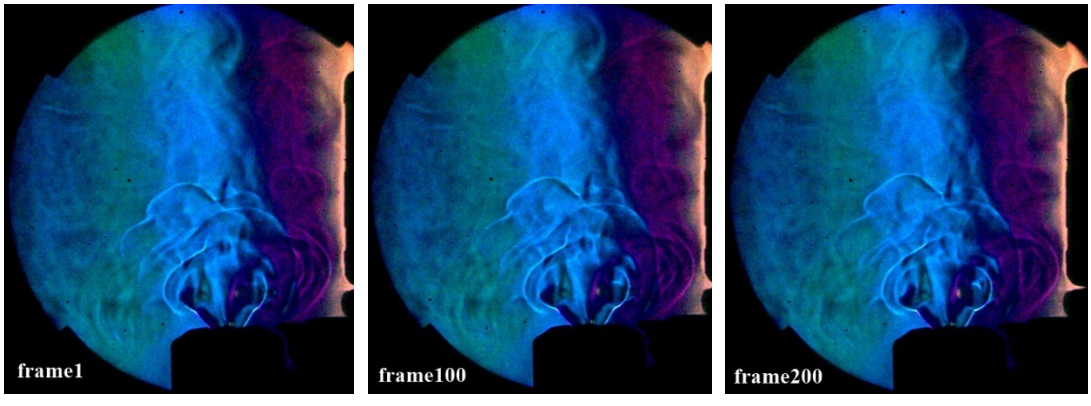

Fig. 4 – Image sequence of the phenomena captured at 7500 fps

3.1 Application of the SIV technique

As mentioned in the introductory section, SIV mainly uses the same tracking principle as the PIV technique. The post-processign software used here is the commercially available PIVlab. Velocity vectors, cross correlation coeficient and vorticity maps are generated for the images containing the phenomena, in a time-resolved manner. Table 3 presents a selection of algoirthms typically used in PIV analysis.

Table 3. Typical parameters used in PIV analysis

Parameter name	Parameter specifics
PIV algorithm deployed	FFT window deformation
Sub-pixel estimator	Gaus 2x3 - point
Interrogation area	64x64, 16x16
Interrogation steps	16x16, 8x8
Correlation robustness	Standard
Calibration process	x-increases towards right y-increases towards bottom
ROI	Selected to contain the entire phenomenon
Number of analysed frames	200
Digital anemometer	Wintact WtT87

A short assessment of the FFT and DIC methods is conducted below. In the field of fluid dynamics and thermal analysis, particularly in the visualization of heat transfer and density gradients using schlieren techniques, both fast Fourier transform (FFT) and digital image correlation (DIC) are pivotal in the post-processing of experimental data. These methods offer distinct approaches to the analysis of particle displacement and flow dynamics captured in schlieren images, providing complementary insights into the behavior of near- laminar flames, such as those observed in the thermal plume of a candle.

FFT is particularly effective in calculating the correlation between successive images by transforming them into the frequency domain. This approach, as detailed by Raffel et al. [16], is computationally efficient and excels at determining average particle displacements across large datasets. FFT's strength lies in its ability to quickly process large-scale image data, making it suitable for applications requiring rapid and broad analyses of fluid dynamics. Conversely, DIC operates in the spatial domain, comparing pixel intensities directly between image pairs to calculate displacement fields with high precision. DIC is known for its accuracy in capturing minute deformations and particle movements within each image, as described by Sutton et al. [18]. This method is particularly beneficial for detailed flow analysis, allowing for a more granular understanding of how subtle changes in the thermal plume of a candle affect overall flow dynamics.

The comparative study of these methods, such as those by Dalziel et al. [19] and Westerweel [20], highlights that while FFT provides a broader, more efficient analysis suitable for initial data processing, DIC offers higher precision in tracking the complex, small-scale movements within the fluid flow, making it invaluable for detailed studies of laminar flames.

Notably, works by Scarano [21] and Keane & Adrian [22] further elaborate on the applicability of these methods in Particle Image Velocimetry (PIV) analysis, providing insights into their effectiveness in different experimental setups. Scarano emphasizes the importance of selecting appropriate correlation methods depending on the scale and nature of

the flow being studied, while Keane & Adrian discuss the benefits of hybrid approaches that combine the efficiency of FFT with the precision of DIC.

Additionally, the implementation of these techniques in MATLAB's PIVlab, as demonstrated in the studies by Thielicke & Stamhuis [23] and Willert & Gharib [24], showcases how modern software tools can be leveraged to refine and optimize the post-processing of schlieren images. These tools enable the creation of detailed velocity maps and temperature distributions, which are crucial for advancing the understanding of thermal plumes in nearly laminar flames.

By integrating the strengths of both FFT and DIC, this research enhances the visualization and analysis of a candle's thermal plume, offering new insights into the flow dynamics of nearly laminar flames.

The dual application of these methods allows for a more comprehensive study of the fluid mechanics involved, contributing to the broader field of experimental fluid dynamics and thermal analysis. For a better understanding of the post-processing algorithm, a logical scheme is provided in Fig. 5.

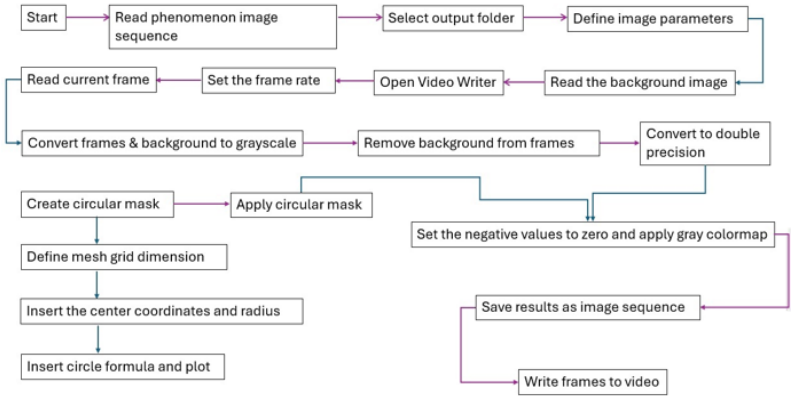

Fig. 5 – Post processing MATLAB algorithm steps

There are 4 post-processing sessions performed on the image sequence containing the phenomenon. The analysis has been achieved over 5 frames in the sequence, namely frame 1, 50, 100, 150 and 200. The recording speed has exceeded the variations found in the phenomenon, given its laminar tendency. The specifications of the 4 sessions can be found in Table 4 and were firstly used in [25].

Table 4. Settings used to compare each derivative parameter in post processing sessions [25]

Ses. no.	Nb. of passes	Interrogation window area vs. interrogation step	Analysis Method	Subpixel interpolator	Other specifications	Derivative parameters checked
1	3	a) 64x32; 32x16; 16x8; b) 32x16; 16x8; 8x4	FFT	Gauss 2x3-point	Magnification factor: 1px=4.1637e-04m Coordinates: - x increases towards the right - y increases towards the top	- U component - V Component - Correlation coefficients
2	2	64x32; 32x16;	FFT			
3	1	32x16	DCC			
4	1	64x32;	DCC	2D Gauss		

The results of this analysis are presented in section 4, together with the results from the colorimetry study.

3.2 A brief schlieren colorimetry study of the image sequence

Integrating colorimetry with schlieren techniques, results in higher image resolution and more informative visualizations of aerodynamic and fluid dynamic phenomena, improving the accuracy of flow characterization and analysis.

The use of the segmented filter in the present study allows for the determination of the observable density range which is strongly correlated to the schlieren system's sensitivty. The temperature distribution of a candle frame is presented in Fig. 6. However, the zones captured by the schlieren color system are defined through the color displacement in the image plane. Fig. 6 -b) represents a colored schlieren image useful in the computational process, despite of not having a great contrast or a strong visual impact on the observant.

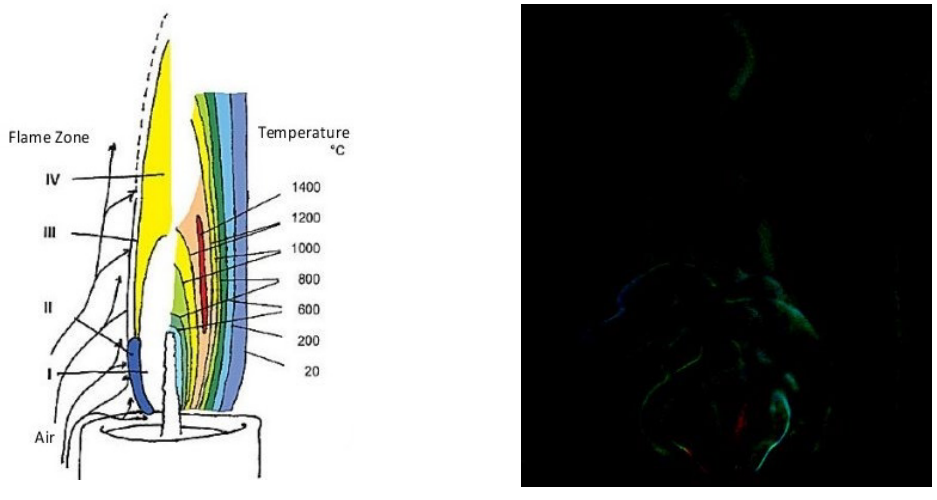

a) b)

Fig. 6 – a) Typical temperature distribution in a wax candle flame [26], b) displacement of the color distribution generated by the filter in the candle flame images, after background extraction

The steps of post-processing colorimetry data included in the Matlab algorithm are: background removal, normalizing image sequence and assessment of color displacement. When observing the image sequence depicted in Fig. 4, it can be observed that one element is intruding the test area. The high-speed camera which, given the positioning of the mirrors with reduced off axis angle, intrudes the plume of the candle flame.

Despite this intrusion, the effects on the experimental data is null, as the camera and its dissipated heat are easily removed in an image averaging process. The temperature range of the flame is presented in chapter 4 and conclusions regarding the experimental campaign and its results, are contained in chapter 5.

4. RESULTS

4.1 Results from the SIV analysis

From the SIV analysis, several graphs have been extracted. The first parameter analysed is the the velocity determined on the u and v components. The x component represents the centre line of the candle flame, starting from the wick and reaching the superior vertical limit of the flame image. It increases with the distance from the candle wick, while y increases from left to right. The resulting vector maps for the sessions 1-3 applying FFT, from table 4 are presented in Fig. 7.

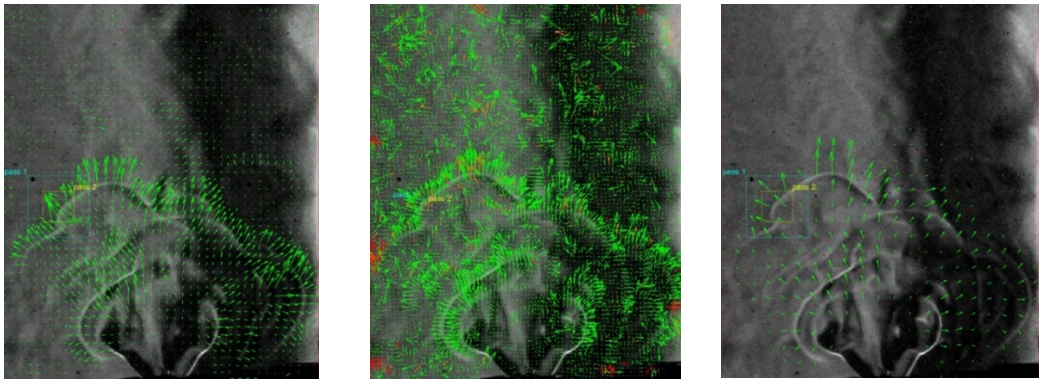

a) b) c)

Fig. 7 – Vector maps for: a) session 1 -a., b) session 1-b and c) session 2, from Table 4

The results from the DIC method named DCC in PIVlab are not included as the vector map has a poor spatial resolution resulting in inconclusive data. Fig. 8 and Fig. 9 present the graphs obtained for the sessions, for the u and respectively u component of the velocity. The data is extracted for comparison from 3 horizontal lines placed in the vector field. The first line is represented in Fig. 8 a)−c), the second horizontal line is presented in d)−f), and the third line is represented by g)−i) points. The same arrangement follows Fig. 9, where the *u*-component is presented.

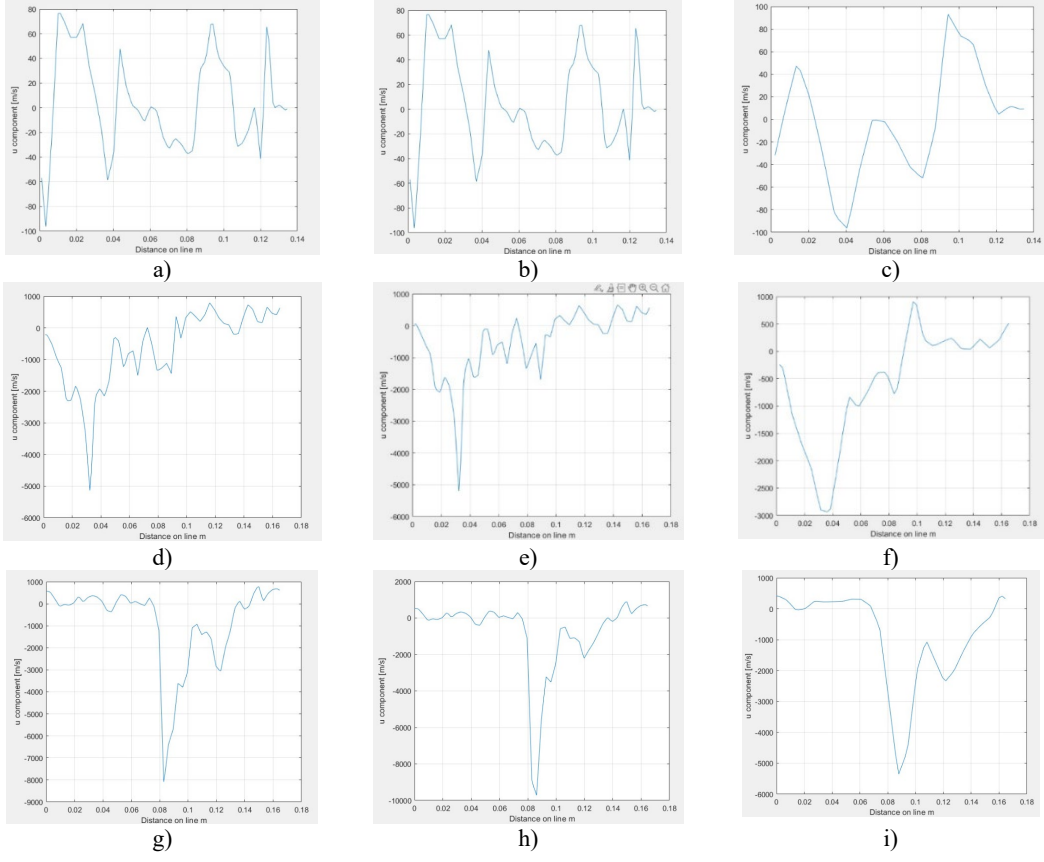

a) b) c)

d) e) f)

g) h) i)

Fig. 8 – *u* component for:- wick horizontal line a) session 1 -a., b) session 1-b and c) session 2, 2nd horizontal line: d) session 1-a., e) session 1-b and f) session 2, 3rd line: g) session 1-a., h) session 1-b and i) session 2

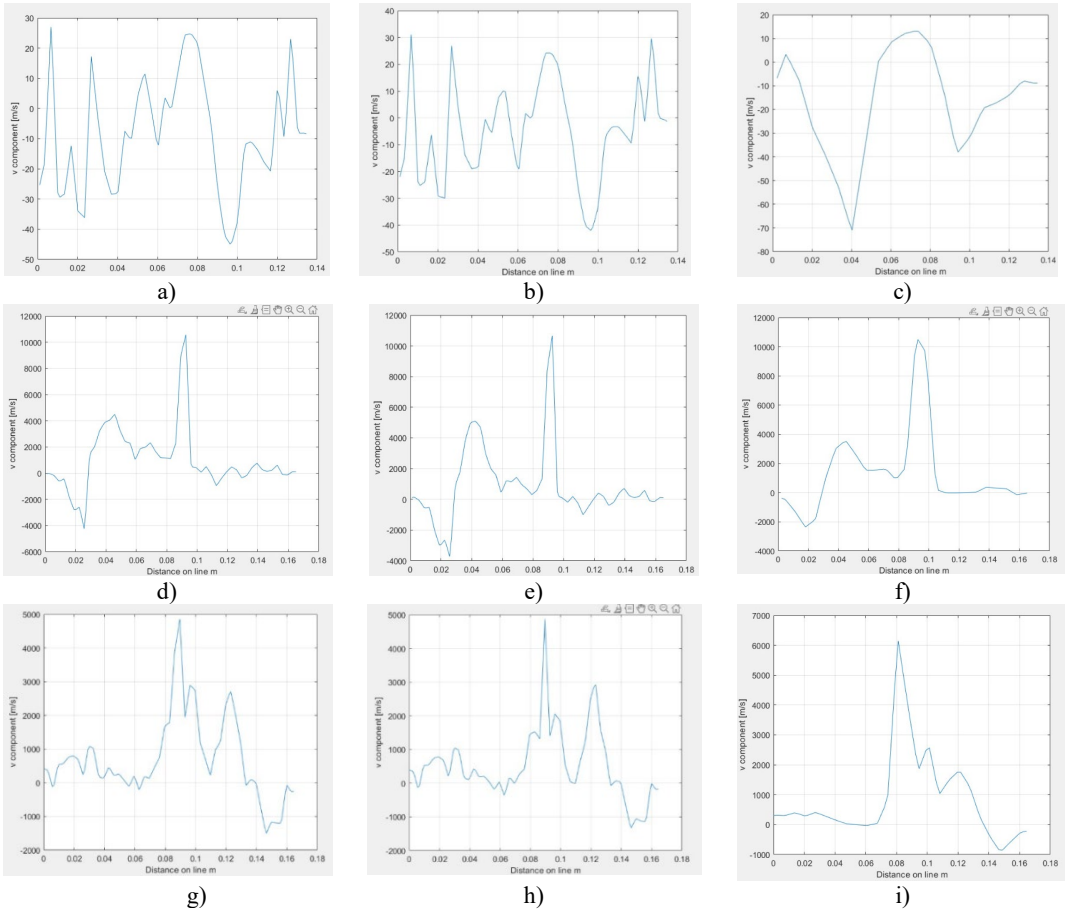

Fig. 9 – u component for:- wick horizontal line a) session 1 -a., b) session 1-b and c) session 2, 2nd horizontal line: d) session 1-a., e) session 1-b and f) session 2, 3rd line: g) session 1-a., h) session 1-b and i) session 2

For analysing the cross-correlation's spatial resolution, Fig. 10 depicts the cross-correlation coefficient maps for a) session 1-b and b) session 2. It can be observed that by applying a single interrogation step, the spatial resolution increases substantially.

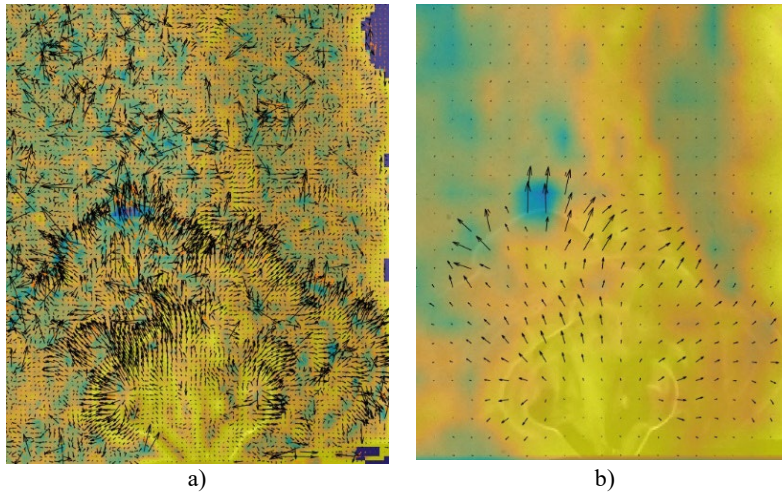

Fig. 10 Cross−correlation coefficient for: a) – session 1b and b) session 2

4.2 Results of the colorimetry approximation

The color filter schlieren method is used in this case, as explained before, to extract density gradients. The filter is firstly mapped by translating every point of it over the source image. Having broader color fringes, like in the present case, can lead to having color gradient displacement contained only within the initial background image. This will lead to the observation of only large density differences between the environment and the candle.
The density gradients are found with the Gladstone-Dale equation [27], found in (1).

$$\boldsymbol{n = 1 + K \cdot \rho} \tag{1}$$

where n is the refractive index, K is the Gladstone-Dale constant and ρ represents density.
Density values are extracted from the refractive index obtained. The refracted index is calculated from the deflection angle known for every pixel. The deflection angle, ε, is found with equation (2), where d represents the displacement of the color gradient onto another pixel, f_2 represents the focal length of the second parabolic mirror and x_1 is the distance from the focal point of the second parabolic mirror and the camera sensor. ε is approximated to have the same value as its tangent, which is genarally the case for very small angles.

$$tan\varepsilon = \frac{d}{f_2 + x_1} \qquad [14] \tag{2}$$

A threshold is fixed for each post-proceesed image, pixels closed to black are replaced with value 0. This helps Matlab identify only the pixels that need to be analysed. Further steps include a tracking function, applied to all the non-black pixels, available for post processing. The RGB channels are flattened into a 2D matrix where each pixel's RGB values are stored in adjacent columns. Afterwards, the positions of the analysed pixels are introduced in the same table. The table is read in Matlab and the pixels are linked to those found in the background image. The result is a table with the displacements of each color gradient, containing their new pixel adress. After the displacement has been found, (2) is applied, and the values are converted into densities.
The present study uses the equation of state (3) to derive the temperature range of the flame.

$$T = \frac{PM}{\rho R} \qquad [28] \tag{3}$$

where T is the temperature of an ideal gas, P is the pressure, rho is the density and R is the gas constant. Ocnsidering this as an ideal gas introduces a large range of errors. However, the paper is basing its claims on the schlieren method an less on the exact calculation of the chemistry parameters. Fig. 11 presents in a graphical way the resulted temperature range.

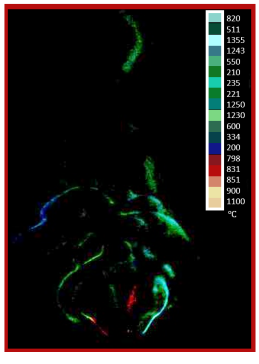

Fig. 11 Resulted temperature range

The image processing step revealed a color pattern. Nuances not found on the filter have been eliminated in order to not affect the depiction of the results.

5. CONCLUSIONS

Applying SIV methods to a turbulent-like candle flame allows for the determination of velocity fields using commercially available software. Among the sessions analyzed, Session 2—with the settings detailed in Table 4—yields more accurate velocity vectors. However, this session suffers from lower spatial resolution compared to other cross-correlation sessions that use three interrogation steps. A balance between spatial resolutions and processing time is recommended when using PIVlab in schlieren techniques.

As the accuracy of the velocity vectors increases, so does the occurrence of spurious vectors, making manual selection and rejection increasingly tedious. This challenge can be mitigated by capping velocity limits, which helps eliminate both high-magnitude vectors, likely caused by cross-correlation errors, and low-magnitude vectors, which are often irrelevant background noise.

In colorimetry analysis, the primary conclusion is that while a comprehensive temperature map can be derived from the images, a significant compromise must be made between filter size, manufacturing method, and the width of the colored fringes. Larger filter sizes require longer calibration times, and in this study, the filters shown in Fig. 1 and Fig. 3 were manually crafted from optical filters [29]. For optimal analysis, the fringe width should be submicron in scale. The purpose of this colorimetry analysis was to demonstrate the feasibility of the concept. However, colorimetry demands substantial computational power for image analysis, image acquisition, and color interpretation, all of which are necessary for accurately calculating temperature values.

This paper shows that SIV methods can determine velocity fields in a turbulent-like candle flame, with Session 2 providing the most accurate vectors despite lower spatial resolution. Balancing resolution and processing time is crucial, and capping velocity limits can reduce errors. The colorimetry analysis confirms the feasibility of creating temperature maps, though it demands high computational power and careful filter design.

ACKNOWLEDGEMENT

This work was carried out through the “Nucleu” Program, within the framework of the National Plan for Research, Development, and Innovation 2023–2026, supported by the Romanian Ministry of Research, Innovation, and Development, project number PN23.12.01.02. The author would like to extend their gratitude to the Romanian Research and Development Institute for Gas Turbines, COMOTI, for providing the necessary equipment and the invaluable opportunity to learn and gain practical experience during the internship program. Their support and resources were instrumental in the successful completion of this research. ChatGpt 4.0 was used for language improvement purposes only.

REFERENCES

[1] G. S. Settles, *Schlieren und shadowgraph techniques: visualizing phenomena in transparent media*, Springer-Verlag Berlin Heidelberg GmbH, Berlin, 1949.

[2] E. Schmidt, Schlierenaufnahmen des temperaturfeldes in der nahe wormeab-gebender korper, *Forschung auf dem Gebiete des Ingenieurwesens*, **3**(4):181–9, 1932

[3] E. G. Prisăcariu, T. Prisecaru, R. E. Nicoară, J. A. Vilag, V. A. Vilag, Velocity mapping of an H2-O2 exhaust

jet in air, by means of Schlieren Image Velocimetry (SIV), *Aerospace*, vol. **10**(7), 2023.
[4] H. Schardin, Das toeplersche schlierenverfahren: Grundlagen fur seine anwendung und quantitative auswertung, *VDI-Forschungsheft* No. 367, 5(4):1–32, 1934.
[5] G. E. A. Meier, *Hintergrund schlierenmessverfahren*, Deutsche Patentanmeldung, 1999.
[6] W. Howes, Rainbow schlieren and its applications, *Applied Optics*, **23**(14):2449–60, 1984.
[7] A. Agrawal, N. Butuk, S. Gollahalli, Three-dimensional rainbow schlieren tomography of a temperature field in gas flows, *Applied Optics*, **37**:479–85, 1998.
[8] R. J. Adrian, M. Gharib, W. Merzkirch, D. Rockwell, J. H. Whitelaw, *Experimental Fluid Mechanics*, Springer, 2003.
[9] G. S. Settle, D. R. Jonassen, Schlieren "PIV" for turbulent flows, *Optics and Lasers in Engineering*, **44**(3):190-207, 2003.
[10] D. R. Philpott, A variable sensitivity and orientation colour schlieren system, *Experiments in Fluids*, **29**:42–442, 2000.
[11] A. Martínez-González, D. Moreno-Hernández, J. A. Guerrero-Viramontes, M. León-Rodríguez, J. C. I. Zamarripa-Ramírez, C. Carrillo-Delgado Temperature measurement of fluid flow by using a focusing schlieren method, *Journal of Advanced Optical Techniques*, **15**, 123-134, 2024.
[12] * * * Online, URL: https://www.bhphotovideo.com/c/browse/kodak-gelatin-wratten-filters/ci/7632, Accessed 5th of April 2024
[13] J. Klinge, M. L. Riethmuller, Segment-based and background-oriented schlieren techniques for detailed flow visualization, *Applied Optics*, **41**, 2951-2964, 2002.
[14] G. E. Elsinga, B. W. van Oudheusden, F. Scarano, D. W. Watt, Assessment and application of quantitative schlieren methods: Calibrated color schlieren and background oriented schlieren, *Journal of Flow Visualization and Image Processing*, **55**, 101-123, 2024.
[15] E. G. Prisacariu, T. Prisecaru, Schlieren image velocimetry methods for a round, hot, turbulent air-jet, *INCAS BULLETIN*, (print) ISSN 2066–8201, (online) ISSN 2247–4528, ISSN–L 2066–8201, vol **15**, issue 3, pp. 75-88, 2023, https://doi.org/10.13111/2066-8201.2023.15.3.6
[16] M. Raffel, C. Willert & F. Scarano, *Particle Image Velocimetry: A Practical Guide*, Springer, 2018.
[17] * * * Online, URL: https://www.youtube.com/watch?v=15RTs_USHFk, Accessed: 7th of June 2024.
[18] M. A. Sutton, J. J. Orteu & H. W. Schreier, Image Correlation for Shape, Motion and Deformation Measurements: Basic Concepts, *Theory and Applications*, Springer, 2009.
[19] S. B. Dalziel, G. O. Hughes & B. R. Sutherland, Whole-field density measurements by 'synthetic schlieren', *Experiments in Fluids*, **28**(4), 322-335, 2000.
[20] J. Westerweel, Fundamentals of digital particle image velocimetry, *Measurement Science and Technology*, **8**(12), 1379-1392, 1997.
[21] F. Scarano, Iterative image deformation methods in PIV, *Measurement Science and Technology*, **13**(1), R1-R19, 2002.
[22] R. D. Keane & R. J. Adrian, Theory of cross-correlation analysis of PIV images, *Applied Scientific Research*, **49**(3), 191-215, 1992.
[23] W. Thielicke & E. J. Stamhuis, PIVlab – Towards User-friendly, Affordable and Accurate Digital Particle Image Velocimetry in Matlab, *Journal of Open Research Software*, **2**(1), e30, 2014.
[24] C. Willert & M. Gharib, Digital Particle Image Velocimetry, *Experiments in Fluids*, **10**(4), 181-193, 1991.
[25] E. G. Prisăcariu, SIV for an RTJ, using a PIV commercially available post-processing software, *Turbo Journal*, vol. **10** (1), pp. 25-45, 2023.
[26] * * * Online, URL: https://www.chemistryviews.org/details/ezine/1369631, Accessed 7th of April 2024.
[27] Z. Gao, P. Song, Y. Wang, Y. Su, Refractive index measurement of gas flows using the Gladstone-Dale relation with background-oriented Schlieren, *Applied Optics*, **58**(14), pp. 3775-3782, 2019.
[28] * * * Online, URL: https://www.grc.nasa.gov/www/k-12/airplane/eqstat.html, Accessed 7th of June 2024.
[29] * * * Online, URL: https://www.f64.ro/godox-ad-s11-s12-flash-color-gel-pack-reflector-grid/p, Accessed 2nd of May 2024.